Immunity, Vol. 13, 703–714, November, 2000, Copyright ©2000 by Cell Press

Deletion of Germline Promoter PDβ1 from the TCRβ Locus Causes Hypermethylation that Impairs Dβ1 Recombination by Multiple Mechanisms

Charles E. Whitehurst,* Mark S. Schlissel,† and Jianzhu Chen*‡

*Center for Cancer Research and Department of Biology
Massachusetts Institute of Technology
Cambridge, Massachusetts 02139

†Department of Molecular and Cell Biology
University of California, Berkeley
Berkeley, California 94720

Summary

The role of the germline transcriptional promoter, PDβ1, in V(D)J recombination at the T cell receptor β locus was investigated. Deletion of PDβ1 caused reduced germline transcription and DNA hypermethylation in the Dβ1-Jβ1 region and decreased Dβ1 rearrangement. Analyses of methylation levels surrounding recombination signal sequences (RSS) before, during, and after recombination revealed that under physiological conditions cleavage of hypomethylated alleles was preferred over hypermethylated alleles. Methylation of a specific CpG site within the heptamer of the 3′ Dβ1 RSS was incompatible with cleavage by the V(D)J recombinase. These findings suggest that methylation can regulate V(D)J recombination both at a general level by influencing regional chromatin accessibility and specifically by blocking RSS recognition or cleavage by the V(D)J recombinase.

Introduction

The variable exons of antigen receptor genes are assembled from variable (V), diversity (D), and joining (J) gene segments by a process referred to as V(D)J recombination (Tonegawa, 1983). Lymphocyte-specific RAG1 and RAG2 proteins bind to recombination signal sequences (RSS) catalyzing a cleavage reaction producing hairpin coding ends and blunt phosphorylated signal ends (Gellert, 1997). Ubiquitously expressed proteins involved in double-stranded break repair complete the recombination reaction by processing and ligating the generated ends (Grawunder et al., 1998). Recombination of all antigen receptor genes uses the same V(D)J recombinase and conserved RSS; therefore, the lineage-, stage-, and allele-specificity of recombination is regulated by controlling RSS accessibility to the common V(D)J recombinase (Yancopoulos et al., 1986; Schlissel and Stanhope-Baker, 1997).

RSS packaged within nucleosomes are inaccessible to cleavage by the V(D)J recombinase in vitro (Kwon et al., 1998; Golding et al., 1999; McBlane and Boyes, 2000). Therefore, V(D)J recombinational accessibility is thought to require the perturbation of normal nucleosomal structure. Endogenous RSS accessibility is controlled by *cis* regulatory elements positioned within antigen receptor genes (Schlissel and Stanhope-Baker, 1997), with transcriptional enhancers exerting control over large regions of antigen receptor loci (Chen et al., 1993; Demengeot et al., 1995; Bories et al., 1996; Bouvier et al., 1996; McMurry et al., 1997) and germline (g.l.) transcriptional promoters targeting accessibility to proximal gene segments (Villey et al., 1996; Sikes et al., 1999; Whitehurst et al., 1999; Ye et al., 1999). DNA demethylation and histone acetylation are both events tightly coupled to transcriptional and recombinational accessibility, and both are thought to influence higher order chromatin structure (Mostoslavsky and Bergman, 1997; Eden et al., 1998; Cedar and Bergman, 1999; Cherry and Baltimore, 1999; Jones and Wolffe, 1999; Mathieu et al., 2000; McBlane and Boyes, 2000; McMurry and Krangel, 2000). Several studies have clearly shown transcriptional enhancers to be involved in establishing hypomethylated and hyperacetylated antigen receptor loci (Chen et al., 1993; Lichtenstein et al., 1994; Kirillov et al., 1996; Mostovslavsky et al., 1998; Mathieu et al., 2000; McMurry and Krangel, 2000); however, whether g.l. transcriptional promoters are required to target these modification events to specific gene segments is not known. Moreover, although the developmentally programmed demethylation of antigen receptor loci temporally correlates with the onset of recombination (Mostoslavsky and Bergman, 1997), it remains unclear whether hypomethylation is essential for establishing endogenous RSS accessibility to the V(D)J recombinase.

We previously demonstrated that deletion of 3.6 kb of DNA from the *TCR*β locus (ΔPD3), which contained the PDβ1 g.l. promoter, and two additional DNase I hypersensitive sites, HS10 and HS11, severely impaired both g.l. transcription from and rearrangements of the Dβ1 gene segment, whereas transcription from and rearrangement of the distal Dβ2 gene segment was unaffected (Whitehurst et al., 1999). We have now delineated the role of PDβ1 alone in controlling g.l. transcription, DNA demethylation, histone H3 acetylation, and V(D)J recombination by deleting the minimal 390 bp core region of this promoter (ΔPD) and comparing these mice with ΔPD3 mice. Our findings demonstrate that (1) PDβ1 is required for targeting the normal demethylation and recombinational accessibility of the Dβ1 region, but not the Dβ2 region; (2) *cis* elements upstream of PDβ1 (HS10 and HS11) contribute to Dβ1 recombinational accessibility; (3) RSS cleavage of hypermethylated alleles occurs but is disfavored compared to hypomethylated alleles; and (4) methylation of a CpG in the heptamer of the 3′ RSS of Dβ1 is incompatible with cleavage by the recombinase.

Results

PDβ1 Deletion Impairs Dβ1 Rearrangement, Accessibility to the V(D)J Recombinase, and Associated Histone H3 Acetylation

We generated mice in which a 390 bp EcoNI-AccI fragment corresponding to the core PDβ1 region was de-

‡To whom correspondence should be addressed (e-mail: jchen@mit.edu).

leted (ΔPD) (Figure 1A; see Experimental Procedures for details). The TATA box in the upstream RSS of Dβ1 and the associated transcription initiation sites are left intact (Sikes et al., 1998; Whitehurst et al., 1999). Thymocyte development and T cell maturation in homozygous ΔPD and ΔPD3 mice were normal because of functional Vβ to Dβ2Jβ2 rearrangement (Figure 2). Both mutations were bred onto a RAG2-deficient background (ΔRAG) allowing studies of the g.l. *TCR*β allele at the $CD4^{-}CD8^{-}CD44^{-}CD25^{+}$ thymocyte stage (DN) when the *TCR*β locus is poised for recombination and eliminating complications due to differential rearrangements. Northern blotting of total RNA from DN thymocytes of mice on a ΔRAG background demonstrated that the ΔPD and ΔPD3 mutations resulted in a 10- and 500-fold reduction in g.l. transcripts initiating from Dβ1, respectively, whereas Dβ2 g.l. transcripts were not significantly altered (Figures 1B and 1C).

*TCR*β rearrangement was examined by a Southern blotting assay. Whole thymus DNA was digested with HindIII and hybridized with a probe from the Dβ1-Jβ1 intervening region (probe A), permitting discrimination of wild-type (WT) (8.9 kb) and ΔPD (6.7 kb) alleles (Figure 1D). Because any Dβ1 rearrangement deletes the intervening region, causing loss of hybridization, the hybridization signal is inversely correlated with Dβ1 rearrangement level. The 8.9 kb g.l. fragment was detected in kidney DNA but barely detectable in thymocyte DNA (Figure 1D; upper panel, lanes 1 and 2), consistent with nearly complete Dβ1 rearrangement in thymocytes. Both WT and ΔPD alleles were detected at equal intensities in heterozygous kidney DNA, but in thymic DNA the WT allele was undetectable, whereas a substantial level of ΔPD allele was detected (Figure 1D, lanes 3 and 4). The 6.7 kb ΔPD fragment was also detected in homozygous ΔPD thymocyte DNA (Figure 1D, lanes 5 and 6). The above results were not caused by differences in DNA quantities loaded per lane as shown by rehybridization of the same filter with probe XP.8, which hybridizes to a region 20 kb downstream of Vβ14 that is not subjected to recombination. Probing with a Dβ2-Jβ2.1 intervening fragment revealed no differences in Dβ2 rearrangement between WT and mutant alleles (Figure 1D, lower panel).

Specific Dβ to Jβ rearrangements were measured by semiquantitative PCR assays using primers annealing upstream of Dβ1 and downstream of Jβ1.5. In kidney DNA of ΔRAG mice, only g.l. fragments were amplified (Figure 2A, lane 2). In WT thymic DNA, no g.l. fragments were amplified, but coding joints corresponding to all possible Dβ1 to Jβ1 rearrangements were detected (Figure 2A, lanes 7 and 8). In ΔPD3 thymic DNA, the most abundant products amplified were g.l. fragments, whereas coding joints were reduced 20- to 50-fold compared to WT (Figure 2A, lanes 3, 4, and 7–11). In ΔPD thymic DNA, Dβ1Jβ1 coding joints were present around 5-fold less than WT samples, and g.l. fragments were more abundant than in WT but not as abundant as in ΔPD3 samples (Figure 2A; lanes 5, 6, and 7–11). Dβ1 to Jβ2 coding joints were similarly reduced around 5-fold in thymic DNA of ΔPD mice (data not shown). In contrast, Dβ2 to Jβ2 coding joints were equally amplified using primers annealing upstream of Dβ2 and downstream of Jβ2.6 from each of the thymic DNA samples (Figure 2A).

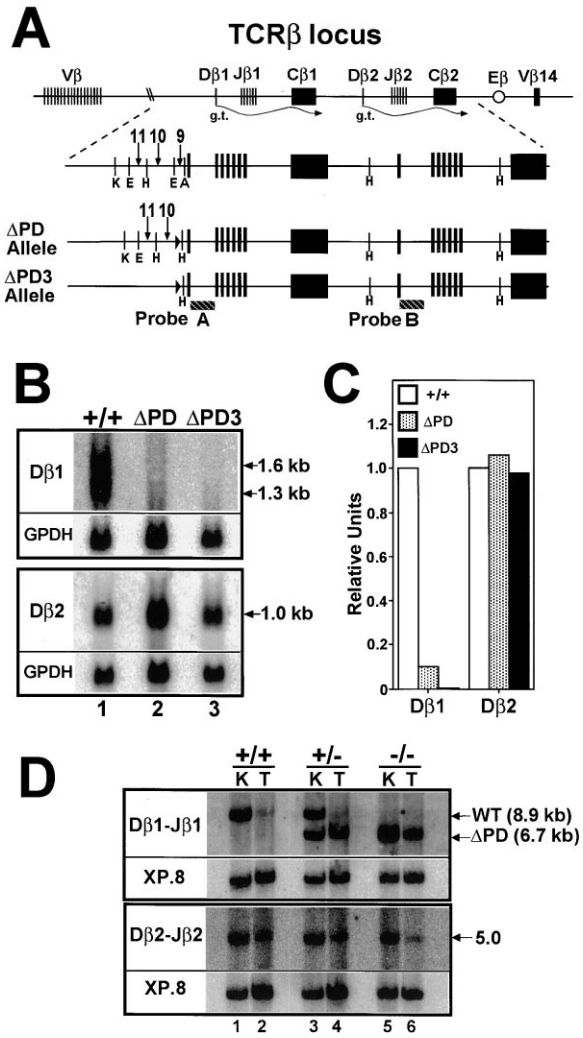

Figure 1. Effect of Targeted Deletion of PDβ1 on g.l. Transcription and V(D)J Recombination of *TCR*β

(A) Schematic diagram of murine *TCR*β and ΔPD and ΔPD3 alleles generated after homologous recombination and Cre-mediated deletion of floxed *neo* gene. On the ΔPD3 allele, DNase I hypersensitive sites (HS) 9, 10, and 11 were deleted, whereas on the ΔPD allele only HS9 was deleted, which corresponds to the core PDβ1 promoter. A, AccI; K, KpnI; E, EcoNI; and H, HindIII. The AccI site is 15 nucleotides upstream of the 5′ RSS of Dβ1 and is replaced by a HindIII site.

(B) Northern analysis of Dβ1 (probe A) and Dβ2 (probe B) region g.l. transcripts in WT (+/+), ΔPD, and ΔPD3 DN thymocytes from mice on a ΔRAG background. Filters were stripped and reprobed with a glyceraldehyde phosphodehydrogenase (GPDH) probe to control for loading.

(C) Bar graph of relative transcript levels determined by phosphorimager analyses of data in (B).

(D) Southern analyses for Dβ1-Jβ1 and Dβ2-Jβ2 rearrangement in wild-type and heterozygous and homozygous ΔPD mice. HindIII-digested DNA from kidney (K) and thymus (T) were electrophoresed on 0.8% agarose, blotted to membranes, and hybridized with probe A (Dβ1-Jβ1) or B (Dβ2-Jβ2). Membranes were stripped and reprobed with XP.8 to quantify DNA loaded per lane.

Vβ12 to Dβ1Jβ1 and Dβ2Jβ2 rearrangements were similarly examined using seminested PCR reactions. While all possible Vβ12Dβ1Jβ1 coding joints were abundantly detected in DNA of WT thymus (Figure 2A; lanes

7 and 8), only a few Vβ12Dβ1Jβ1 products at much lower levels were detected in ΔPD and ΔPD3 thymic DNA (lanes 3–6). We estimated VβDβ1Jβ1 coding joints in ΔPD and ΔPD3 thymic DNA were less than 5% of those in WT samples by comparing serial dilutions of WT thymic DNA into ΔRAG kidney DNA (lanes 9–11). In contrast, levels of Vβ12Dβ2Jβ2 coding joints were similar in WT, ΔPD, and ΔPD3 thymic DNA (Figure 2A). Therefore, compared to ΔPD3, the ΔPD mutation results in the same, albeit less severe, impairments in Dβ1 rearrangement.

The relative impairments in Dβ1 rearrangement in ΔPD and ΔPD3 thymocytes correlated with inaccessibility of the 3′ Dβ1 RSS to cleavage by the V(D)J recombinase as demonstrated by RAG1/RAG2-mediated in vitro cleavage assays utilizing nuclei derived from mice on a ΔRAG background (Stanhope-Baker et al., 1996). As shown in Figure 2B, 3′ Dβ1 signal break ends (SBE) were readily measurable in WT nuclei in a RAG-dependent manner (lanes 1 and 2), whereas in ΔPD and ΔPD3 nuclei these SBE were ~4-fold (lanes 3 and 4) and 20-fold (lanes 5 and 6) less abundant, respectively. In contrast, 3′ Dβ2 SBE were similarly detected in the WT, ΔPD, and ΔPD3 nuclei (Figure 2B, lower panel).

Several studies have provided evidence that accessible RSS are associated with chromatin having hyperacetylated histones (Durum et al., 1998; McBlane and Boyes, 2000; McMurry and Krangel, 2000). Therefore, we performed chromatin immunoprecipitation (ChIP) assays to determine whether the reduced Dβ1 rearrangement and accessibility in ΔPD and ΔPD3 thymocytes was associated with corresponding decreases in histone H3 acetylation. Nuclei from DN thymocytes of the designated mice on a ΔRAG background were fixed with formaldehyde and sonicated to generate chromatin preparations from which acetylated H3 was immunoprecipitated. Cross-linked DNA associated with the acetylated H3 was then liberated and used as a template for semiquantitative PCR assays. In WT thymocytes, a considerable fraction of Dβ1 and Jβ1.1 gene segments were associated with acetylated H3, whereas there was much less association by the inactive gene *Oct-2* (Figures 2D and 2E). The 20% reduction in H3 acetylation associated with Dβ1 and Jβ1.1 in ΔPD compared to WT thymocytes was not significant because a similar reduction was observed for *Oct-2*. A significant level of reduction (50%) in H3 acetylation at Dβ1 and Jβ1.1 was observed in ΔPD3 thymocytes. In contrast, the levels of H3 acetylation at Dβ2 were elevated in ΔPD and ΔPD3 thymocytes compared to WT (Figures 2D and 2E). Thus, reduced Dβ1 accessibility to the V(D)J recombinase in ΔPD3 thymocytes correlates with reduced H3 acetylation of chromatin associated with Dβ1, whereas such a correlation is not clearly demonstrable in ΔPD thymocytes.

PDβ1 Deletion Results in Hypermethylation of the Dβ1 Region

DNA associated with repressed or inaccessible chromatin is typically hypermethylated. In vertebrates, DNA methylation occurs on the cytosine of CpG dinucleotides. Relative to surrounding DNA, CpG dinucleotides were enriched in the Dβ1 and Dβ2 regions (Figure 3A). Given the reduced accessibility of Dβ1 in ΔPD and ΔPD3 thymocytes, we next examined DNA methylation in the Dβ1 region. DNA from kidney and thymocytes of heterozygous (+/ΔPD and +/ΔPD3) mice on ΔRAG backgrounds were digested with HindIII alone or in combination with three methylation-sensitive endonucleases (SmaI, NaeI, or BsrBI) and assayed by Southern blotting with probe A. HindIII digestion generated 8.9 kb (WT) and 6.7 kb (mutant) fragments (Figures 3B and 3C), allowing simultaneous monitoring of WT and ΔPD, or ΔPD3 alleles. Addition of XmaI, a methylation-insensitive isoschizomer of SmaI, yielded the expected restriction fragments of 3.3 and 1.2 kb for the WT and mutant alleles, respectively. HindIII plus SmaI showed that both WT and mutant alleles in kidney DNA were equally resistant to digestion and therefore were equally hypermethylated. In thymus DNA, over 85% of the WT allele was digested by SmaI, indicating hypomethylation. In contrast, ΔPD and ΔPD3 alleles were more resistant to SmaI (60% and 20% digested, respectively), demonstrating hypermethylation. Similarly, in thymus the ΔPD and ΔPD3 alleles were more resistant to NaeI (50% and 10% digested) compared to the WT allele (75%). Interestingly, both WT and ΔPD alleles in the thymus were similarly sensitive (80%) to BsrBI, whereas the ΔPD3 allele was more resistant (65%).

We extended our study by assaying additional CpG sites utilizing the methylation-sensitive single nucleotide primer extension assay (Ms-SNuPE), a method not dependent on methylation-sensitive endonuclease sites (Gonzalgo and Jones, 1997). In this assay, DNA is first treated with bisulfite to convert cytosine to uracil, whereas methylated cytosines are resistant to bisulfite conversion (Figure 4A; Clark et al., 1994). The treated DNA is then amplified by PCR so that uracil becomes thymidine (T), whereas cytosine (C) remains the same. The ratio of C versus T at a given CpG site is measured by a single nucleotide primer extension assay using the same PCR product and an identical primer that anneals just upstream of the C or T, except that one tube contains [α^{32}P]dCTP and the other [α^{32}P]TTP. If proper base complementarity exists, labeled C or T is added to the primer after a single Taq-based extension step. The labeled primers are separated by polyacrylamide gel electrophoresis and then quantified, allowing the calculation of the percentage of methylation at the assayed CpG site. Thus, the methylation at a given CpG site is reflected by the ratio of C versus T in the PCR product. Unlike bisulfite sequencing analysis for DNA methylation, Ms-SNuPE does not directly show *cis* relationships of the methylation status of adjacent CpGs.

We first assayed the methylation of six CpG sites in the Dβ1 region (Figure 4B) and determined the accuracy of Ms-SNuPE by titrating kidney DNA into thymus DNA from a ΔRAG mouse. All sites were hypermethylated in kidney and hypomethylated in thymus (Figure 4C). Ms-SNuPE accurately detected increasing methylation corresponding with the titration of increasing kidney DNA into thymus DNA (Figures 4C and 4D). Comparison of three sites assayed by Ms-SNuPE (CpG #1105, 1151, and 2694) and restriction enzymes (SmaI, NaeI, and BsrBI) showed that the methods correlated well (Figure 5C). Although Ms-SNuPE gave a higher overall methylation at CpG #2694 than BsrBI digestion in all DNA prepa-

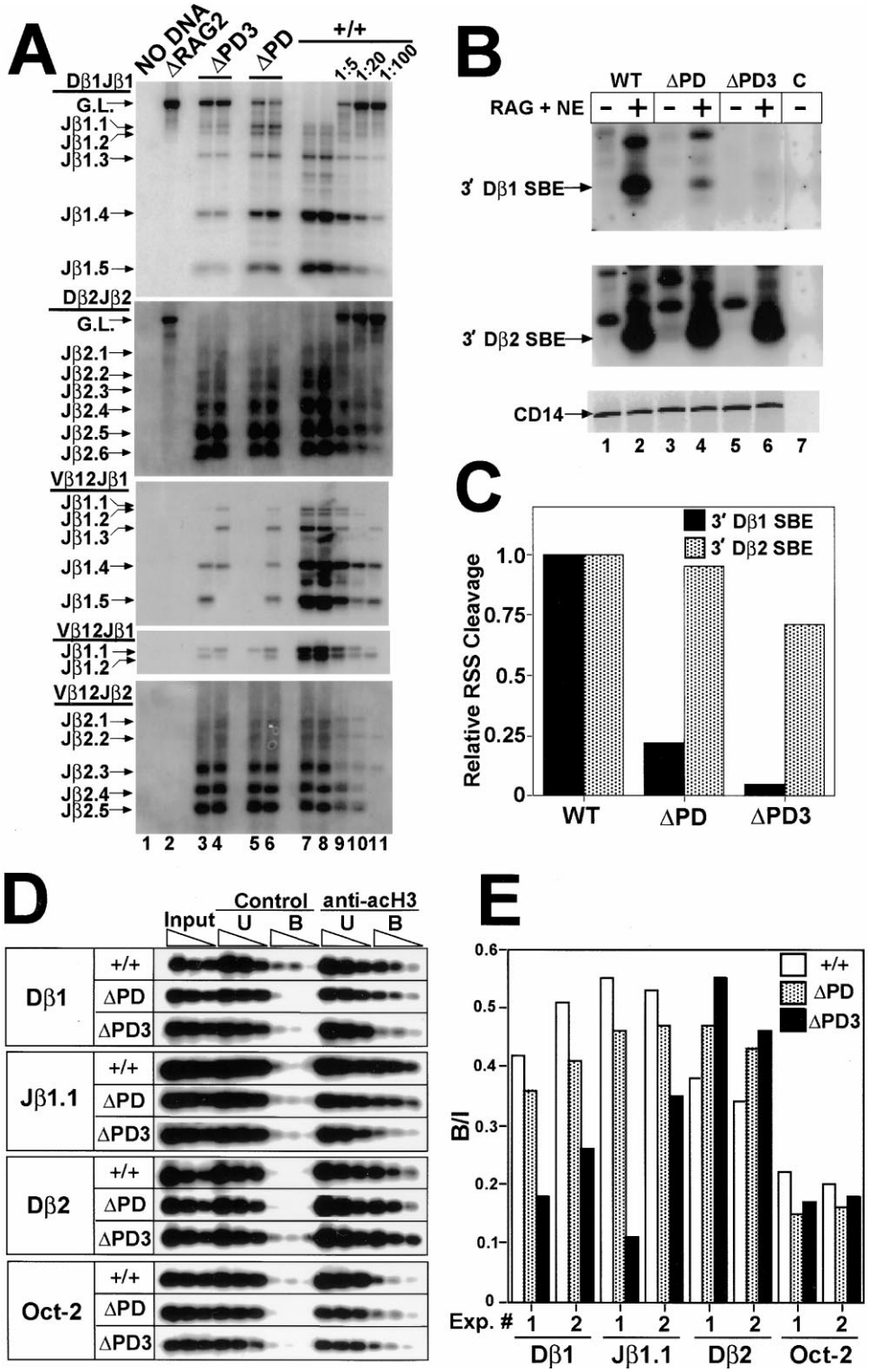

Figure 2. Comparison of Effects of ΔPD and ΔPD3 Mutations on Dβ1 Rearrangements, Accessibility to the V(D)J Recombinase, and Associated Histone H3 Acetylation

(A) Semiquantitative PCR assays measuring specific *TCR*β rearrangements. DNA used was from total thymocytes of WT (+/+) and homozygous ΔPD or ΔPD3 mice or from kidney of ΔRAG2 mice. Thymocyte DNA from two mice of each genotype was assayed. For relative quantitative comparisons, WT thymus DNA was diluted 1:5, 1:20, and 1:100 into ΔRAG2 kidney DNA (lanes 9–11). Individual rearrangements are labeled. G.L., germline fragment.

(B) In vitro RAG-mediated cleavage assay measuring 3′ Dβ1 and Dβ2 RSS accessibility. Nuclei were isolated from WT and homozygous mutant mice on a ΔRAG background and reconstituted with recombinant RAG1 and 2 proteins and calf thymus nuclear extract (NE) and the

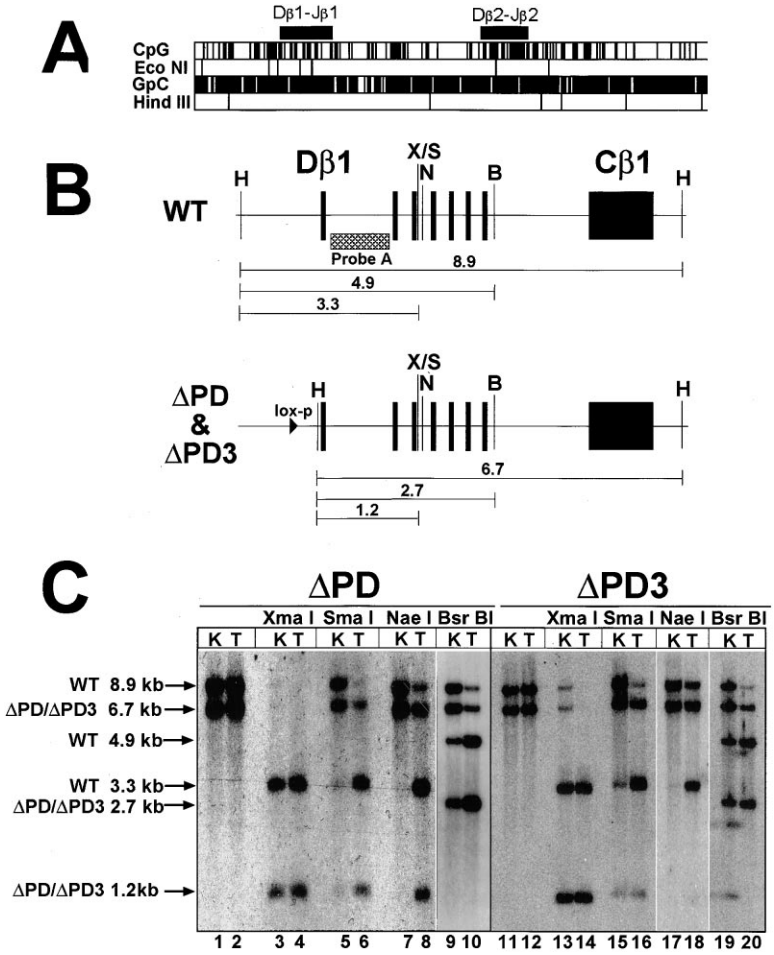

Figure 3. Comparison of the DNA Methylation Status of WT, ΔPD, and ΔPD3 Alleles Using Methylation-Sensitive Restriction Enzymes

(A) Map showing density of CpG sites in Dβ1/Jβ1 and Dβ2/Jβ2 regions of *TCR*β. EcoNI and HindIII sites are reference points. The HindIII fragment containing the Dβ1/Jβ1 region is 8.9 kb. PDβ1 lies within the EcoNI sites upstream of Dβ1.

(B) Map showing restriction sites at the Dβ1/Jβ1 region of the WT, ΔPD, and ΔPD3 alleles and enzymes and probes used for Southern analyses. ΔPD and ΔPD3 alleles are physically identical downstream of the lox-p site. H, HindIII; X, XmaI; S, SmaI; N, NaeI; and B, BsrBI. Sizes shown are in kb. Probe A is the same as in Figure 1A.

(C) Southern analyses of kidney (K) and thymocyte (T) DNA digested with HindIII alone or plus one of the methylation-sensitive restriction enzymes and hybridized with probe A. XmaI has the same recognition site as SmaI but is methylation insensitive. DNA in all lanes was from heterozygous ΔPD or heterozygous ΔPD3 mice on a homozygous ΔRAG2 background.

rations, this may reflect insensitivity of the site to bisulfite conversion or the possibility that cleavage by BsrBI is not completely blocked by DNA methylation. Thus, Ms-SNuPE is a reliable quantitative method for measuring DNA methylation as previously shown (Gonzalgo and Jones, 1997).

Using Ms-SnuPE, we compared methylation of nine CpG sites, seven in the Dβ1 region and two in the Dβ2 region, in kidney and thymus DNA from WT, ΔPD, and ΔPD3 mice on a ΔRAG background (Figure 5A). All sites were hypermethylated in kidney (66%–94%) and hypomethylated in WT thymus DNA (13%–44%; Figure 5B). In contrast, the two sites nearest Dβ1 (CpG #9 and 743) were hypermethylated (85%–95%) in ΔPD thymus at a level equivalent to that observed in kidney (89%–92%). The next five sites (CpG #1105, 1151, 1914, 2598, and 2694) in the Dβ1 region were also more methylated in ΔPD thymus (26%–50%) as compared to WT thymus (13%–26%) but not as hypermethylated as in kidney. In DNA from ΔPD3 thymus, all sites in the Dβ1 region were hypermethylated (81%–97%) at the same levels as in kidney. Two sites in the Dβ2 region (CpG #9371 and 9651) were equivalently hypomethylated in WT, ΔPD, and ΔPD3 thymus (Figure 5B), and the same was found for four additional sites in that region (data not shown). Therefore, deletion of PDβ1 causes hypermethylation of the Dβ1 region to different extents depending on the size of the deletion, whereas the Dβ2 region is unaffected.

Additional CpG sites (>70% of all possible sites) in a 4 kb region containing Dβ1 and Jβ1 gene segments were assayed by Ms-SNuPE, allowing construction of a map that more clearly delineated the methylation changes caused by the ΔPD and ΔPD3 mutations (Figure 6A). The percentages of methylation of all 37 CpG sites assayed by Ms-SNuPE were plotted versus their respective positions. In WT kidney, all CpG sites were hyper-

generated signal ends (SBE) measured by ligation-mediated PCR as previously described (Stanhope-Baker et al., 1996; Whitehurst et al., 1999). CD14 was amplified as a control for DNA template consistency.

(C) Bar graph of relative 3′ Dβ1 and Dβ2 SBE levels measured by phosphorimager analyses of (C).

(D) Representative ChIP experiments measuring histone H3 acetylation in the designated *TCR*β regions or the control gene *OCT-2* in DN thymocytes of WT and homozygous mutant mice on a ΔRAG background. DNA isolated from unbound (U) and bound (B) chromatin fractions were serially diluted 3-fold before they were used as template for PCR amplification.

(E) Graphical representation of two separate ChIP experiments measuring H3 acetylation in designated *TCR*β regions. Data represent the ratio of (anti-H3 bound)/(input).

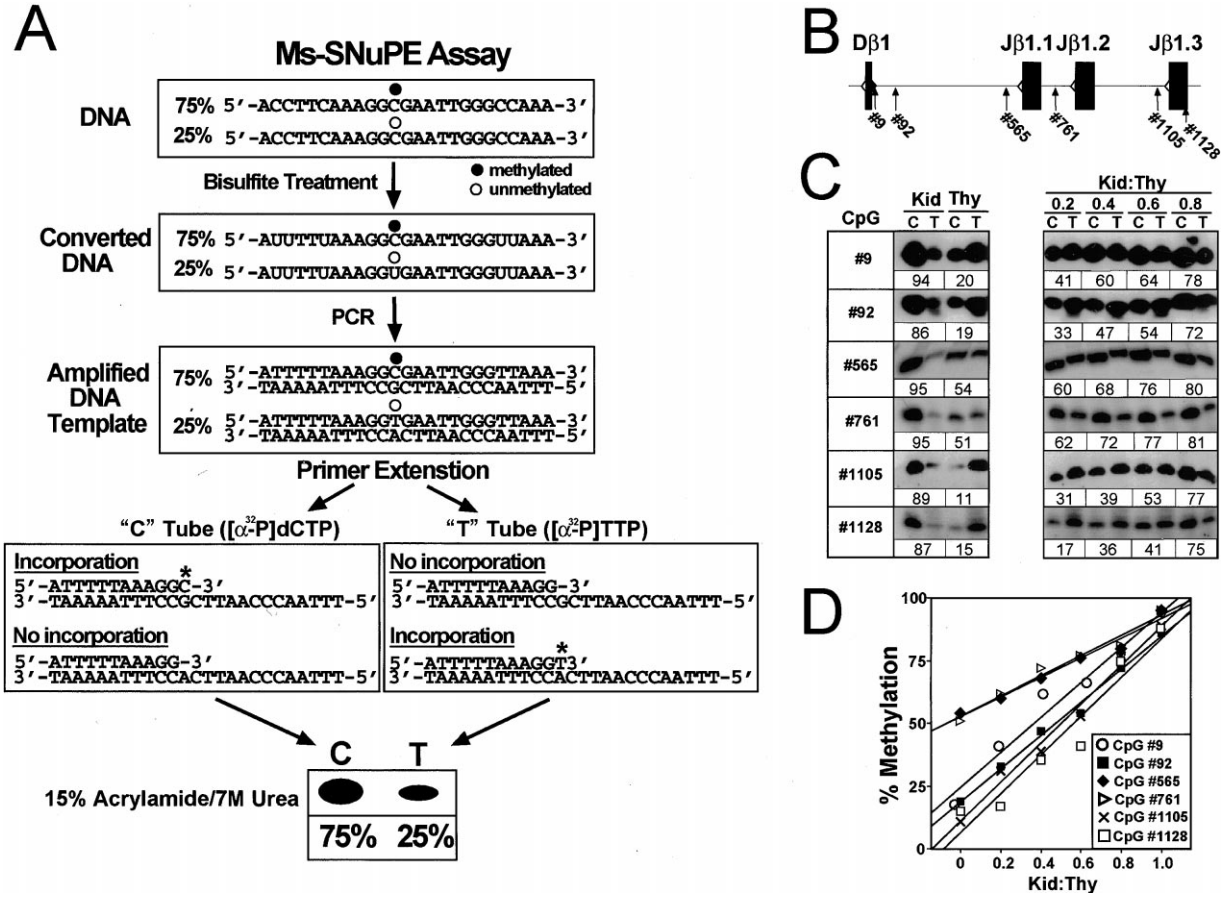

Figure 4. Quantitative Assessment of Ms-SNuPE Assay for DNA Methylation in Dβ1 Region

(A) Schematic summary of Ms-SNuPE assay assuming that 75% of the CpG site is methylated. Only the sense strand is shown.

(B) Location of six CpG sites in the Dβ1 to Jβ1.3 region at which methylation was measured. Numbers represent the positions of the sites relative to the Dβ1 gene segment (see Experimental Procedures). CpG #1105 corresponds to the same site as measured by SmaI digestion in Figure 3.

(C) Ms-SNuPE assays measuring methylation status of CpG sites shown in (B). The left panel represents assays in kidney (Kid) and DN thymocyte (Thy) DNA from ΔRAG mice. The right panel (Kid:Thy) represents a titration wherein increasing amounts of kidney DNA was mixed with DN thymocyte DNA prior to Ms-SNuPE assay. Reactions were resolved on 15% denaturing polyacrylamide gels, and the emitted radioactivity was measured by phosphorimager. “C” indicates methylation and “T” indicates no methylation. The number below each “C T” represents the percentage methylation of the assayed CpG.

(D) A plot of data in (C) showing linear relationship between increasing percentage of CpG methylation and increasing amount of kidney DNA in kidney:thymus mixtures. On the graph axis zero reflects 100% thymus DNA and 1.0 reflects 100% kidney DNA. The correlation coefficients calculated for the experiments were all over 0.98.

methylated (60%–95%), whereas in WT thymus all sites except those upstream of PDβ1 were hypomethylated (5%–55%), with methylation levels always less than kidney. The domain of hypomethylation started ~250 base pairs upstream of the PDβ1 core promoter and extended over 0.5 kb downstream of the Jβ1.6 gene segment (4 kb). In ΔPD thymus, all CpG sites upstream of the deleted PDβ1 core promoter remained hypermethylated at levels similar to kidney, as did all CpG sites in approximately a 1 kb region immediately downstream of the Dβ1 gene segment (Figure 6A). However, progressively downstream from the Jβ1.2 gene segment the CpG sites became more hypomethylated until no apparent differences in methylation were observed between the WT and ΔPD thymus beyond the Jβ1.4 gene segment. In ΔPD3 thymus DNA, all but two CpG sites were hypermethylated at a level similar as in kidney (Figure 6A). The two oddly hypomethylated CpG sites, located just downstream of Jβ1.4, were hypermethylated in kidney, demonstrating that the sites are capable of being methylated in other tissues. This complexity in the methylation profiles of the two mutants clearly underscores the importance of assaying multiple CpG sites in a locus to accurately assess the DNA methylation status. These findings suggest that PDβ1 and probably additional elements upstream of PDβ1 as revealed by the ΔPD3 mutation target efficient demethylation in the Dβ1 region during T cell development.

Assessment of DNA Methylation Surrounding RSS before, during, and after Recombination

Although the ΔPD and ΔPD3 mutations resulted in abnormal hypermethylation of the Dβ1 region and a concomitant impairment in Dβ1 rearrangement, neither

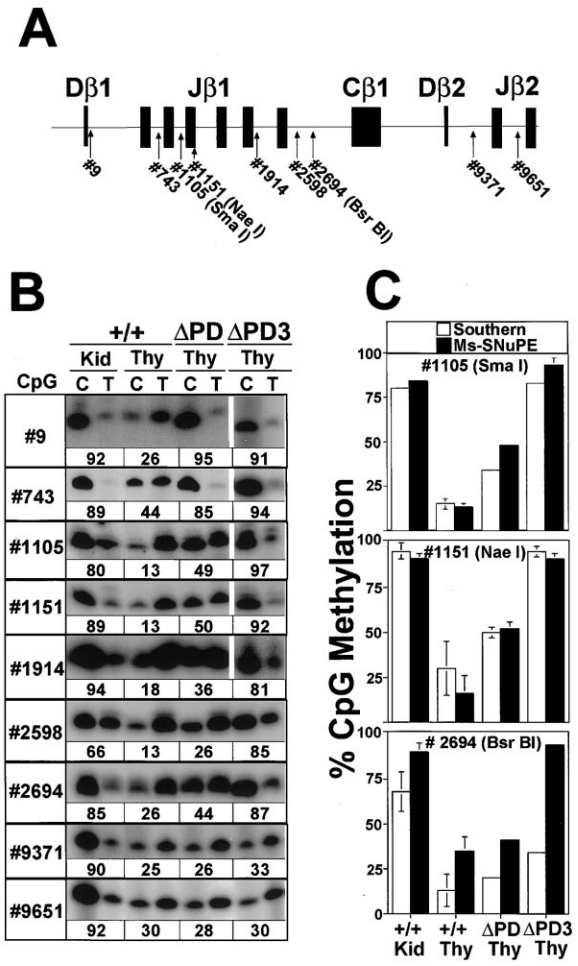

Figure 5. Quantification of the DNA Methylation of Nine CpG Sites on WT, ΔPD, and ΔPD3 *TCR*β Alleles by Ms-SNuPE

(A) Map showing positions of nine CpG sites in *TCR*β at which methylation was measured.

(B) Representative Ms-SNuPE assays showing methylation status of the nine CpG sites in kidney (Kid) DNA, and WT and homozygous mutant (ΔPD and ΔPD3) thymus (Thy) DNA from mice on a ΔRAG background.

(C) Comparison of the methylation levels of three CpG sites (CpG #1105, #1151, and #2694) measured by methylation-sensitive restriction digestion (Figure 3 and data not shown) and Ms-SNuPE (Figure 4C and 5B). Mean and standard deviation (error bars) of data from at least two assays quantified by phosphorimager analyses are shown.

hypermethylation nor blockage in rearrangement was absolute. Therefore, we performed experiments to measure at what level hypomethylation was required for Dβ1 rearrangement on the ΔPD and ΔPD3 alleles. We first examined the methylation status immediately before and after rearrangement of two CpG sites associated with the Jβ1.3 gene segment (Figure 6B) by using DNA isolated from purified DN thymocytes of WT (+/+) and mutant (ΔPD or ΔPD3) mice on a normal or ΔRAG background (Figures 6B and 6C). The two CpG sites were hypomethylated (32% and 20%) in g.l. WT DNA, whereas they were more methylated (63% and 45%) in g.l. ΔPD DNA and were hypermethylated (93% and 91%) in g.l. ΔPD3 DNA (Figure 6D). In contrast, these same CpG sites were similarly hypomethylated in Dβ1Jβ1.3 coding joints in DNA preparations from WT, ΔPD, and ΔPD3 thymocytes.

Although these findings suggested that rare Dβ1 to Jβ1 rearrangements in mutant thymocytes preferentially occurred on hypomethylated alleles, it remained possible that demethylation occurred during or immediately after Dβ1Jβ1.3 coding joint formation. Therefore, we performed the ligation-mediated Ms-SNuPE assay (LM-MsSNuPE) to determine the methylation status of CpG sites associated with the rare signal ends (SBE) formed in the mutant thymocytes. Because SBE are transient intermediates formed directly by RAG-mediated cleavage (Schlissel et al., 1993; Gellert, 1997), the methylation state of DNA associated with SBE most likely reflects the level of methylation permissible to the V(D)J recombinase. If the V(D)J recombinase is inhibited by hypermethylation, then one would expect the rare SBE formed in the mutant thymocytes to be primarily derived from the rare hypomethylated alleles in the population. We assayed three CpG sites, two closely linked with the 3′ Dβ1 SBE (#92 and #129) and one with the Jβ1.3 SBE (#1105) (Figures 7A and 7B). DNA from DN thymocytes of WT and mutant mice on a normal (RAG^+) background were ligated with a linker and then treated with sodium bisulfite. Converted SBE were amplified by PCR and assayed by Ms-SNuPE. For comparison, methylation at the three sites in DNA from DN thymocytes of +/+ and mutant mice on the ΔRAG background was assayed using the normal Ms-SNuPE assay. Consistent with previous Ms-SNuPE data (Figure 6A), all three CpG sites were relatively hypomethylated (<25%) on the g.l. WT allele, whereas they were hypermethylated (>80%) on the g.l. mutant alleles, except that CpG #1105 was partially methylated (40%) in ΔPD mice (Figure 7B). Interestingly, while all three sites associated with SBE from both the WT and mutant DN thymocytes were significantly less methylated than their respective g.l. alleles, it was nevertheless apparent that methylated alleles were also accessible to the V(D)J recombinase (Figures 7B and 7C). We sequenced forty-six cloned LM-MsSNuPE PCR products originating from the 3′ Dβ1 SBE from three separate DN thymocyte DNA preparations (two ΔPD and one ΔPD3) and confirmed that they all had the expected blunt signal ends derived from RAG-mediated cleavage (data not shown). Sequencing also allowed simultaneous assessment of the methylation status of four CpG sites associated with the same 3′ Dβ1 SBE (Figure 7D). The frequency of molecules having three or more of the four CpG sites methylated in *cis* on the same molecule (15%) was significantly less than expected by chance (31%), consistent with the above observation that hypomethylated gene segments are preferentially cleaved by the V(D)J recombinase. It was also clear that molecules having three of the four CpG sites methylated (therefore hypermethylated) were cleaved by the V(D)J recombinase in developing thymocytes. Most strikingly however, CpG #9, which resides within the heptamer of the 3′ Dβ1 RSS (Figure 7E), was unmethylated in all clones sequenced (Figure 7D). Taken together, these findings demonstrate that hypermethylated alleles are disfavored for recombination, and demethylation of CpG #9 appears to be essential for Dβ1 cleavage by the V(D)J recombinase.

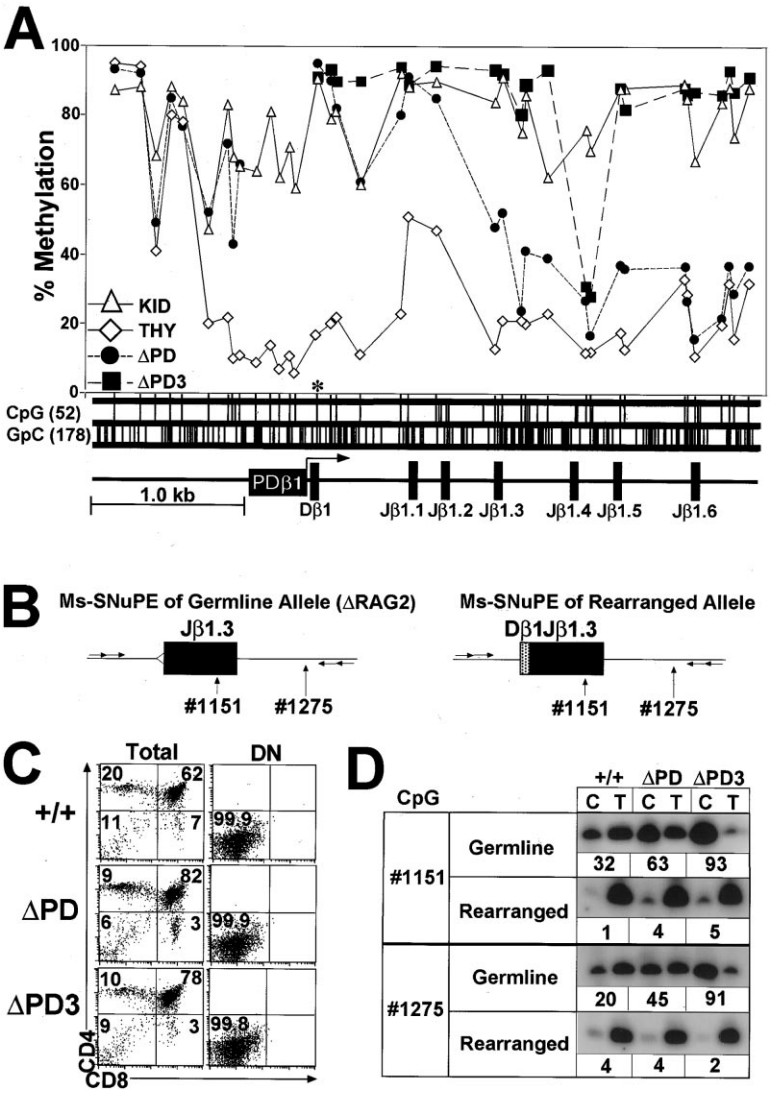

Figure 6. Comparison of the DNA Methylation Profiles of the Dβ1 Region in WT and Mutant Mice and Analyses of Methylation of Dβ1Jβ1.3 Coding Joints in DN Thymocytes of Mutant Mice

(A) DNA methylation at 37 of 52 possible CpG sites (axis of plot) in Dβ1 region as measured by Ms-SNuPE. DNA samples used for Ms-SNuPE assays were isolated from WT kidney (KID), and WT thymus (THY) and homozygous mutant (ΔPD and ΔPD3) thymus from mice all on a ΔRAG2 background. The 390 bp PDβ1 region was only assayed in the kidney and WT thymus samples because it was deleted in the mutant mice, and likewise the entire 3.3 kb region upstream of PDβ1 was not measurable in ΔPD3 mice. The positioning of PDβ1 and the gene segments on the x axis are approximately to scale. The frequencies of GpC dinucleotides are also plotted to allow a relative comparison to CpG density. Each CpG site was assayed at least twice and averages are shown. The starred site represents CpG #9 located in the heptamer of the 3′Dβ1 RSS.

(B) Diagrams showing the g.l. and rearranged configurations of the Jβ1.3 gene segment and the positions of the CpG sites analyzed. Arrows indicate position of PCR primers.

(C) FACS analyses of WT (+/+), ΔPD, and ΔPD3 whole (total) thymocyte populations before and after purification of the DN thymocytes. These DN thymocytes were used for preparing "rearranged" DNA samples for assay of coding joint methylation in (D) and the LM-Ms-SNuPE assays in Figure 7 and were purified from whole thymocyte populations as described (Whitehurst et al., 1999).

(D) Methylation status of CpG #1151 and #1275 associated with the Jβ1.3 gene segment. Unrearranged "g.l." DNA was from DN thymocytes of WT and mutant mice on a ΔRAG background whereas "rearranged" DNA containing Dβ1Jβ1.3 coding joints was derived from the purified DN thymocytes shown in Figure 6C.

Discussion

Our findings demonstrate that PDβ1 is a g.l. transcriptional promoter that functions in specifically targeting the recombinational accessibility of the Dβ1 region. Deletion of the core PDβ1 promoter significantly impairs Dβ1 accessibility to the V(D)J recombinase, as well as g.l. transcription and DNA demethylation. Its role in H3 acetylation is unclear and it may function cooperatively with upstream elements as indicated by the significantly reduced H3 acetylation in ΔPD3 mice. Because deletion of the Eβ enhancer also impairs the above activities (Bories et al., 1996; Bouvier et al., 1996; Mathieu et al., 2000), our findings imply that interactions between PDβ1 and Eβ are required to target Dβ1 accessibility to the V(D)J recombinase and to promote associated g.l. transcription, DNA demethylation, and chromatin remodeling.

The effected chromatin changes at the Dβ1 region caused by the ΔPD3 mutation were more severe than those caused by ΔPD, suggesting additional *cis* elements upstream of PDβ1 may act in concert with PDβ1 to promote transcriptional and recombinational accessibility. Two likely candidates are HS10 and HS11, which were deleted along with PDβ1 by the ΔPD3 mutation and which correspond to stretches of DNA resembling matrix associating regions (MARs) (Chattopadhyay et al., 1998; data not shown). Although the deletion of MARs adjacent to enhancers at *TCR*β*, IgH*, and *Ig*κ loci did not alter their methylation or recombination (Chattopadhyay et al., 1998; Sakai et al., 1999; Yi et al., 1999), studies with *IgH* and *Ig*κ transgenes suggest MARs can facilitate long-range promoter-enhancer interactions and promote formation of larger regions of hypomethylation (Lichtenstein et al., 1994; Jenuwein et al., 1997; Forrester et al., 1999).

Our detailed methylation study of 4 kb of DNA around Dβ1 in WT, ΔPD, and ΔPD3 mice suggest that PDβ1 and HS10 and HS11 function in establishing the hypomethylated state of the Dβ1 region in precursor thymocytes. These findings bring forth the question of by what mechanism does a g.l. promoter target demethylation? Although demethylation in the Dβ1 region is oriented along the path of g.l. transcription elongation, transcrip-

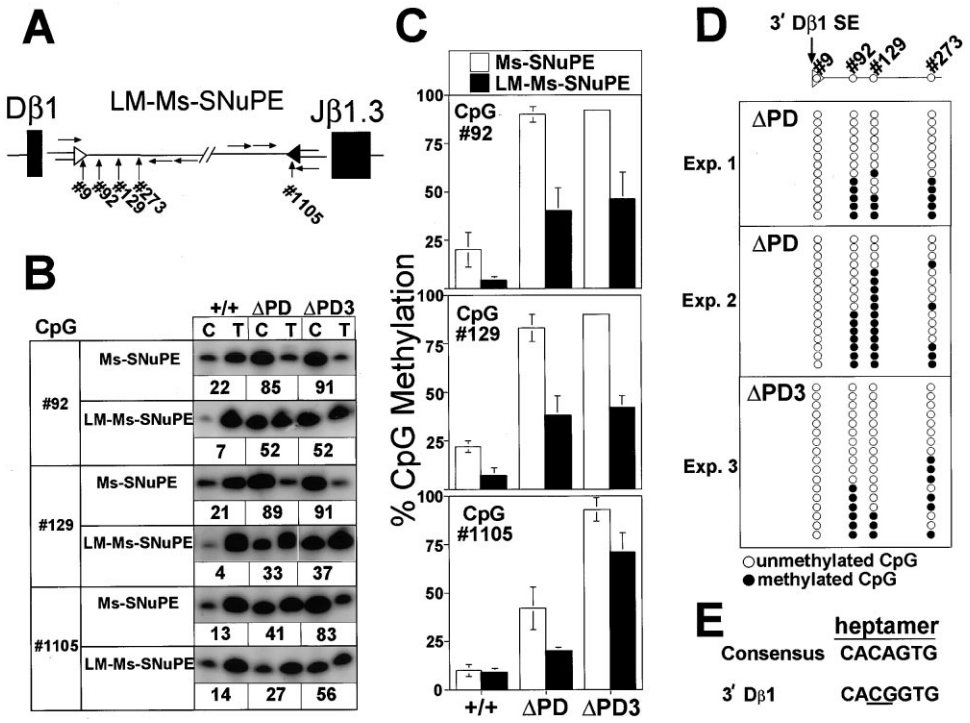

Figure 7. V(D)J Recombinase Activity Is Targeted to Hypomethylated Alleles in ΔPD and ΔPD Mice

(A) Diagram depicting signal ends and locations of associated CpG sites assayed by LM-Ms-SNuPE and sequencing. Arrows indicate position of PCR primers.

(B) Representative experiments showing methylation states of CpG #92, #129, and #1105. Ms-SNuPE was used to measure the methylation in unrearranged "g.l." DNA from DN thymocytes of WT and mutant mice on a ΔRAG background, whereas LM-Ms-SNuPE was used to measure the methylation associated with signal ends from the DNA of purified DN thymocytes (Figure 6C).

(C) Comparison of the methylation levels of the CpG sites shown in (B) measured by Ms-SNuPE to that measured by LM-Ms-SNuPE. Data shown are the means and standard deviations (error bars) calculated from three independent experiments utilizing separately purified populations of DN thymocytes having purity comparable to that shown in Figure 6C.

(D) Methylation status of CpG #9, #92, #129, and #273 determined by sequencing individual cloned PCR products generated from the LM-Ms-SNuPE assay. Each row of circles represents data derived from an individual clone and therefore the methylation status of a single DNA molecule.

(E) Diagram comparing the heptamer sequence of the 3′ Dβ1 RSS to the consensus heptamer sequence. The underlined CpG site corresponds to CpG #9.

tion through a DNA region has not been shown to cause demethylation. Demethylation more likely results from developmentally regulated binding of nuclear factors to *cis* elements that in turn inhibit de novo or maintenance DNA methyltransferases from acting on local CpG sites (Paroush et al., 1990; Matsuo et al., 1998; Hsieh, 1999; Lin et al., 2000). Thus, PDβ1 may target factor binding along the entire Dβ1 region that blocks methylation, or it may function as a boundary element preventing methylation spreading from the flanking upstream region, or it may orient the region in a subnuclear compartment inhibitory to or lacking methyltransferases. Additional studies are required to delineate the molecular mechanism of PDβ1-mediated demethylation.

DNA methylation is thought to inhibit V(D)J recombination indirectly by promoting formation of repressed chromatin structure (Hsieh and Lieber, 1992). Inhibition may involve active recruitment of histone deacetylases associated with repressor complexes containing methyl-CpG binding proteins (Jones and Wolffe, 1999; Ng and Bird, 1999). Like transcriptional initiation (Berger, 1999; Bjorklund et al., 1999), recombination may require regional demethylation and active targeting of histone acetyltransferases by transcription factor binding to g.l. promoters. Our findings along with recent studies have provided support for this model, showing that gene segments that are accessible to the V(D)J recombinase are associated with chromatin having hyperacetylated histones (Durum et al., 1998; Cherry and Baltimore, 1999; Mathieu et al., 2000; McBlane and Boyes, 2000; McMurry and Krangel, 2000). Studies have shown temporal correlations between hypomethylation and V(D)J recombination (Hozumi et al., 1996; Mostoslavsky and Bergman, 1997; Mathieu et al., 2000); however, none have delineated the level of demethylation surrounding a chromatinized RSS required for V(D)J recombinase-mediated cleavage under physiological conditions. We have provided a first glimpse of the physiological amount of DNA demethylation sufficient for accessibility leading to cleavage by the V(D)J recombinase at the Dβ1 region. While hypomethylated alleles are preferentially cleaved and recombined, it is clear that the demethylation of most CpG sites is unessential for cleavage, except for CpG #9 (Figure 7). This observation supports the view

that higher order chromatin structural changes resulting from other events, perhaps histone hyperacetylation, may be primary factors governing recombinational accessibility. By targeting a certain threshhold level of "regional" demethylation and thereby reducing histone deacetylase recruitment, g.l. promoters may augment histone acetylase activities directed to the region by transcription factors and/or chromatin remodeling complexes. Continued demethylation may occur during and after the recombination event to promote subsequent recombination events such as V to DJ rearrangement, as was suggested by progressively increasing hypomethylation observed at the differing stages of recombination (Figure 6D).

Intriguingly, we found that CpG #9 in the heptamer of the 3′ Dβ1 RSS was always demethylated when associated with a SBE. This odd heptamer sequence is conserved in *TCR*β of rat and rainbow trout, but it is not present in human and chicken *TCR*β (De Guerra and Charlemagne, 1997) nor in any other RSS of the remaining murine *TCR*β. Our findings suggest that methylation of CpG #9 perturbs binding and/or cleavage of the 3′ Dβ1 RSS by the V(D)J recombinase, either directly, or indirectly by recruiting methyl-CpG binding proteins. In this scenario, this would represent another level of control of Dβ1 rearrangement in mouse, and perhaps rat and trout, in addition to control exerted by transcription, histone acetylation, and general methylation.

Experimental Procedures

ΔPD Mice

ΔPD J1 ES cells were generated exactly as for ΔPD3 mice (Whitehurst et al., 1999), except that the targeting vector was different, containing a floxed PGK promoter-driven neomycin (*neo*) resistance gene flanked upstream by a 2.9 kb EcoNI homologous fragment and downstream by a 3.8 kb AccI homologous fragment. Homologous recombinant clones were transiently transfected with a CMV-driven Cre expression construct to delete the floxed *neo* gene, leaving a lox-p site in place of PDβ1. DN thymocytes were purified from whole thymocyte populations as described (Whitehurst et al., 1999). Southern blotting and semiquantitative PCR assays to measure *TCR*β rearrangements were performed as described (Whitehurst et al., 1999).

Ms-SNuPE Assays

Ms-SNuPE assays were performed as described (Gonzalgo and Jones, 1997). The assay involves three steps: (1) DNA is treated with bisulfite to convert cytosines to uracils, but 5-methyl-cytosine is resistant to bisulfite and therefore remains cytosines; (2) the bisulfite-treated DNA is purified and used as template for PCR amplification (uracils become thymidines after amplification); and (3) single nucleotide primer extension is then performed on amplified DNA to detect the relative level of methylation (C versus T) at a specific CpG site. A detailed protocol and list of the enzymes and primer combinations used to amplify products from the bisulfite converted DNA are available upon request and from the internet (see supplemental data at http://www.immunity.com/cgi/content/full/13/5/703/DC1). Ms-SNuPE assays were performed on sense strand CpG sites, which are numbered according to their distance in base pairs from the center adenosine residue of the Dβ1 gene segment, with CpG residues upstream of Dβ1 having negative numbers and CpG residues downstream of Dβ1 having positive numbers. Incorporated cytosine (C) corresponds to the amount of methylated cytosine,whereas incorporated thymidine (T) corresponds to the amount of unmethylated cytosine at the CpG site. Therefore, the percentage of methylation (%M) at the assayed CpG site is calculated as % = C/(C + T) × 100. Titration controls were done for six sites shown in Figure 4 but not other sites. The conditions and extension primers used for Ms-SNuPE assays are available upon request and from the internet (http://www.immunity.com/cgi/content/full/13/5/703/DC1). The LM-Ms-SNuPE assay is a combination of the standard ligation-mediated PCR assay commonly used to detected recombination signal ends and Ms-SNuPE (Schlissel et al., 1993). DNA was ligated with a linker, digested with appropriate restriction enzyme and bisulfite converted, and then signal ends were amplified by seminested PCR and products analyzed for methylation by primer extension. In brief, 6 μg of DNA was mixed in a 0.1 ml ligation reaction with 5 U of T4 DNA ligase and 120 pmol of linker (BW-LX, 5′-ataacccagttttctcaaattgctgatagg-3′; and BW-LY, 5′-cctatcag caatttgagaaaactg-3′). After incubation at 25°C for 12–18 hr, the reaction was heat inactivated and phenol/chloroform extracted, and DNA was precipitated by ethanol with 1 μg of glycogen. DNA was then digested with EcoNI, ethanol precipitated and bisulfite converted, and used as a template for PCR amplification. To assess methylation of CpG residues #92 and #129 by MsSNuPE, template was generated by a seminested amplification reaction using sense primer BW-LZ (5′-ataatttagttttttaaattgttgataggta-3′), which only anneals to converted BW-LX/BW-LY linker sequence when it is ligated bluntly to the 3′ SBE of Dβ1, and antisense primers DBM20 (1°; 5′-aattttcctaatcctataataatattcatc-3′) and DBM21 (2°; 5′-caaaacaaa cctataaaactattcacctct-3′), which anneal downstream of Dβ1. For CpG #1105, DNA was similarly ligated with linker (BW-LX1, 5′-ggata gtggttaaagtggtttgattatatt-3′; and BW-LY1, 5′-aaaccactttaaccac tatcc-3′), and template was generated by seminested PCR using antisense primer BW-LZ1 (5′-aatataatcaaaccactttaaccactatccc aca-3′), which anneals to the converted linker sequence when it is ligated bluntly to the SBE of Jβ1.3, and sense primers JBM20 (1°; 5′-attttaatgaggttggatttataaaggtgg-3′) and JBM21 (2°; 5′-aaaggtggat ttattataggtttaggaatg-3′). PCR products used in LM-Ms-SNuPE were cloned into pBluescript KS(-) for sequencing.

Chromatin Immunoprecipitation Assays

Thymocytes from mice on a ΔRAG background were fixed at 5 × 10^6/ml in medium (RPMI-1640, 5% FBS, and 0.5% formaldehyde) for 10 min at 37°C, washed in PBS, and lysed in buffer S (50 mM Tris-HCl [pH 8.1], 10 mM EDTA, 0.5% SDS, 1mM PMSF, 1 μg/ml aprotinin, and 1 μg/ml pepstatin A). Clarified lysate was sonicated 4 × 20 s to generate chromatin preparations averaging 1–3 nucleosomes per particle. ChIP assays were performed using a kit to immunoprecipitate acetylated histone H3 following the manufacturer's protocol (Upstate Biotechnology, Lake Placid, NY). DNA was liberated from H3 and used as template for semiquantitative PCR assays (25 cycles). Products were analyzed by Southern hybridization with radiolabeled probes and phosphorimager analysis. Primers, probes, and conditions to measure OCT-2 were as previously described (McMurry and Krangel, 2000), and primers, probes, and conditions used to measure Dβ1, Jβ1.1, and Dβ2 are available upon request and from the internet at http://www.immunity.com/cgi/content/full/13/5/703/DC1.

Acknowledgments

We thank Ms. Tara Schmidt for generating chimeric mice and other members of the lab for their help and Drs. Phillip Sharp, Yehudit Bergman, and Rudolf Jaenisch for critical review of the manuscript. This work is supported in part by a National Institutes of Health grant AI40146 (to J. C.) and Cancer Research Institute and Merck/Massachusetts Institute of Technology Fellowships (to C. E. W.). M. S. S. acknowledges the support of National Institutes of Health RO1 AI40227 and of a Scholarship from the Leukemia & Lymphoma Society of America.

Received June 2, 2000; revised October 25, 2000.

References

Berger, S.L. (1999). Gene activation by histone and factor acetyltransferases. Curr. Opin. Cell. Biol. *11*, 336–341.

Bjorklund, S., Almouzni, G., Davidson, I., Nightingale, K.P., and Weiss, K. (1999). Global transcription regulators of eukaryotes. Cell *96*, 759–767.

Bories, J.-C., Demengeot, J., Davidson, L., and Alt, F.W. (1996). Gene-targeted deletion and replacement mutations of the T-cell receptor β-chain enhancer: the role of enhancer elements in controlling V(D)J recombination accessibility. Proc. Natl. Acad. Sci. USA *93*, 7871–7876.

Bouvier, G., Watrin, F., Naspetti, M., Verthuy, C., Naquet, P., and Ferrier, P. (1996). Deletion of the mouse T-cell receptor β gene enhancer blocks αβ T-cell development. Proc. Natl. Acad. Sci. USA *93*, 7877–7881.

Cedar, H., and Bergman, Y. (1999). Developmental regulation of immune system gene rearrangement. Curr. Opin. Immunol. *11*, 64–69.

Chattopadhyay, S., Whitehurst, C., Schwenk, F., and Chen, J. (1998). Biochemical and functional analyses of chromatin changes at the TCRβ locus during $CD4^-CD8^-$ to $CD4^+CD8^+$ thymocyte differentiation. J. Immunol. *160*, 1256–1267.

Chen, J., Young, F., Bottaro, A., Stewart, V., Smith, R., and Alt, F. (1993). Mutations of the intronic IgH enhancer and its flanking sequences differentially affect accessibility of the JH locus. EMBO J. *12*, 4635–4645.

Cherry, S.R., and Baltimore, D. (1999). Chromatin remodeling directly activates V(D)J recombination. Proc. Natl. Acad. Sci. USA *96*, 10788–10793.

Clark, S.J., Harrison, J., Paul, C.L., and Frommer, M. (1994). High sensitivity mapping of methylated cytosines. Nucleic Acids Res. *22*, 2990–2997.

De Guerra, A., and Charlemagne, J. (1997). Genomic organization of the TcRβ chain diversity (Dβ) and joining (Jβ) segments in the rainbow trout: presence of many repeated sequences. Mol. Immunol. *34,* 653–662.

Demengeot, J., Oltz, E.M., and Alt, F.W. (1995). Promotion of V(D)J recombinational accessibility by the intronic Eκ element: role of the κB motif. Int. Immunol. *7*, 1995–2003.

Durum, S.K., Candeias, S., Nakajima, H., Leonard, W.J., Baird, A.M., Berg, L.J., and Muegge, K. (1998). Interleukin 7 receptor control of T cell receptor gamma gene rearrangement: role of receptor-associated chains and locus accessibility. J. Exp. Med. *188*, 2233–2241.

Eden, S., Hashimshony, T., Keshet, I., Cedar, H., and Thorne, A.W. (1998). DNA methylation models histone acetylation. Nature *394*, 842.

Forrester, W.C., Fernandez, L.A., and Grosschedl, R. (1999). Nuclear matrix attachment regions antagonize methylation-dependent repression of long-range enhancer-promoter interactions. Genes Dev. *13*, 3003–3014.

Gellert, M. (1997). Recent advances in understanding V(D)J recombination. Adv. Immunol. *64*, 39–64.

Golding, A., Chandler, S., Ballestar, E., Wolffe, A.P., and Schlissel, M.S. (1999). Nucleosomal structure completely inhibits *in vitro* cleavage by the V(D)J recombinase. EMBO J. *18*, 3712–3723.

Gonzalgo, M.L., and Jones, P.A. (1997). Rapid quantitation of methylation differences at specific sites using methylation-sensitive single nucleotide primer extension (Ms-SNuPE). Nucleic Acids Res. *25*, 2529–2531.

Grawunder, U., West, R.B., and Lieber, M.R. (1998). Antigen receptor gene rearrangement. Curr. Opin. Immunol. *10*, 172–180.

Hozumi, K., Kobori, A., Sato, T., Nishimura, T., and Habu, S. (1996). Transcription and demethylation of TCRβ gene initiate prior to the gene rearrangement in c-kit+ thymocytes with CD3 expression: evidence of T cell commitment in the thymus. Int. Immunol. *8*, 1473–1481.

Hsieh, C., and Lieber, M. (1992). CpG methylated minichromosomes become inaccessible for V(D)J recombination after undergoing replication. EMBO J. *11*, 315–325.

Hsieh, C.L. (1999). Evidence that protein binding specifies sites of DNA demethylation. Mol. Cell. Biol. *19*, 46–56.

Kwon, J., Imbalzano, A.N., Matthews, A., and Oettinger, M.A. (1998). Accessibility of nucleosomal DNA to V(D)J cleavage is modulated by RSS positioning and HMG1. Mol. Cell *2*, 829–839.

Jenuwein, T., Forrester, W.C., Fernandez-Herrero, L.A., Laible, G., Dull, M., and Grosschedl, R. (1997). Extension of chromatin accessibility by nuclear matrix attachment regions. Nature *385*, 269–272.

Jones, P.L., and Wolffe, A.P. (1999). Relationships between chromatin organization and DNA methylation in determining gene expression. Semin. Cancer Biol. *9*, 339–347.

Kirillov, A., Kistler, B., Mostoslavsky, R., Cedar, H., Wirth, T., and Bergman, Y. (1996). A role for nuclear NF-kB in B-cell-specific demethylation of the Igκ locus. Nat. Genet. *13*, 435–441.

Lichtenstein, M., Keini, G., Cedar, H., and Bergman, Y. (1994). B cell-specific demethylation: a novel role for the intronic κ chain enhancer sequence. Cell *76*, 913–923.

Lin, I.G., Tomzynski, T.J., Ou, Q., and Hsieh, C.L. (2000). Modulation of DNA binding protein affinity directly affects target site demethylation. Mol. Cell. Biol. *20*, 2343–2349.

Mathieu, M.N., Hempel, W.M., Spicuglia, S., Verthuy, C., and Ferrier, P. (2000). Chromatin remodeling by the T cell receptor (TCR)-β gene enhancer during early T cell development: implications for the control of TCR-β locus recombination. J. Exp. Med. *192*, 625–636.

Matsuo, K., Silke, J., Georgiev, O., Marti, P., Giovannini, N., and Rungger, D. (1998). An embryonic demethylation mechanism involving binding of transcription factors to replicating DNA. EMBO J. *17*, 1446–1453.

McBlane, F., and Boyes, J. (2000). Stimulation of V(D)J recombination by histone acetylation. Curr. Biol. *10*, 483–486.

McMurry, M.T., and Krangel, M.S. (2000). A role for histone acetylation in the developmental regulation of V(D)J recombination. Science *287*, 495–498.

McMurry, M.T., Hernandez-Munain, C., Lauzurica, P., and Krangel, M.S. (1997). Enhancer control of local accessibility to V(D)J recombinase. Mol. Cell. Biol. *17*, 4553–4561.

Mostoslavsky, R., and Bergman, Y. (1997). DNA methylation: regulation of gene expression and role in the immune system. Biochim. Biophys. Acta. *1333*, F29–F50.

Mostoslavsky, R., Singh, N., Kirillov, A., Pelanda, R., Cedar, H., Chess, A., and Bergman, Y. (1998). κ chain monoallelic demethylation and the establishment of allelic exclusion. Genes Dev. *12*, 1801–1811.

Ng, H.H., and Bird, A. (1999). DNA methylation and chromatin modification. Curr. Opin. Genet. Dev. *9*, 158–163.

Paroush, Z., Keshet, I., Yisraeli, J., and Cedar, H. (1990). Dynamics of demethylation and activation of the α-actin gene in myoblasts. Cell *63*, 1229–1237.

Sakai, E., Bottaro, A., Davidson, L., Sleckman, B.P., and Alt, F.W. (1999). Recombination and transcription of the endogenous Ig heavy chain locus is effected by the Ig heavy chain intronic enhancer core region in the absence of the matrix attachment regions. Proc. Natl. Acad. Sci. USA *96*, 1526–1531.

Schlissel, M.S., and Stanhope-Baker, P. (1997). Accessibility and the developmental regulation of V(D)J recombination. Semin. Immunol. *9*, 161–170.

Schlissel, M., Constantinescu, A., Morrow, T., Baxter, M., and Peng, A. (1993). Double-strand signal sequence breaks in V(D)J recombination are blunt, 5′-phosphorylated, RAG-dependent and cell cycle regulated. Genes Dev. *7*, 2520–2532.

Sikes, M.L., Gomez, R.J., Song, J., and Oltz, E.M. (1998). A developmental stage-specific promoter directs germline transcription of DβJβ gene segments in precursor T lymphocytes. J. Immunol. *161*, 1399–1405.

Sikes, M.L., Suarez, C.C., and Oltz, E.M. (1999). Regulation of V(D)J recombination by transcriptional promoters. Mol. Cell. Biol. *19*, 2773–2781.

Stanhope-Baker, P., Hudson, K.M., Shaffer, A.L., Constantinescu, A., and Schlissel, M.S. (1996). Cell type-specific chromatin structure determines the targeting of V(D)J recombinase activity in vitro. Cell *85*, 887–897.

Tonegawa, S. (1983). Somatic generation of antibody diversity. Nature *302*, 575–581.

Villey, I., Caillol, D., Selz, F., Ferrier, P., and de Villartay, J.-P. (1996).

Defect in rearrangement of the most 5′ TCR-Jα following targeted deletion of T early α (TEA): implications for TCRα locus accessibility. Immunity *5*, 331–342.

Whitehurst, C., Chattopadhyay, S., and Chen, J. (1999). Control of V(D)J recombinational accessibility of the Dβ1 gene segment at the TCRβ locus by a germline promoter. Immunity *10*, 313–322.

Yancopoulos, G.D., Blackwell, T.K., Suh, H., Hood, L., and Alt, F.W. (1986). Introduced T cell receptor variable region gene segments recombine in pre-B cells: evidence that B and T cells use a common recombinase. Cell *44*, 251–259.

Ye, S.K., Maki, K., Kitamura, T., Sunaga, S., Akashi, K., Domen, J., Weissman, I.L., Honjo, T., and Ikuta, K. (1999). Induction of germline transcription in the TCRγ locus by Stat5: implications for accessibility control by the IL-7 receptor. Immunity *11*, 213–223.

Yi, M., Wu, P., Trevorrow, K.W., Claflin, L., and Garrard, W.T. (1999). Evidence that the Igκ gene MAR regulates the probability of premature V-J joining and somatic hypermutation. J. Immunol. *162*, 6029–6039.